Neutron and Proton Optical Potentials for
^{12}C, ^{16}O, ^{27}Al, ^{56}Fe, ^{90}Zr and ^{208}Pb up to 250 MeV

Young-Ouk LEE and Jonghwa CHANG
Korea Atomic Energy Research Institute,
Tokio FUKAHORI and Satoshi CHIBA
Japan Atomic Energy Research Institute
e-mail: yolee@lui.kaeri.re.kr

In order to perform nuclear data evaluation without unphysical discontinuities, optical models should cover the whole mass and energy range of interest continuously. In this work, the best set of optical model parameters were obtained with energy dependent potential forms which incorporate effects of dispersion relationship for neutron and proton up to 250 MeV on ^{12}C, ^{16}O, ^{27}Al, ^{56}Fe, ^{90}Zr and ^{208}Pb. Applicability of adopting an identical geometrical factor for the real volume, imaginary volume and imaginary surface potentials has been investigated as well in the process of parameter search.

1. Introduction

Nuclear data for conventional fission reactors and fusion devices mainly consist of neutron-induced cross sections in energy below 20 MeV. However, recent new applications, such as radiation transport simulations of cancer radiotherapy and the accelerator-driven transmutation of nuclear wastes require evaluated nuclear data on neutron- and proton-induced reaction above 20 MeV up to a few GeV.

The optical model provides the basis for theoretical evaluations of nuclear corss sections that are used in providing nuclear data for applications. In addition to offering a convinient means for calculations of reaction, shape elastic, and (neutron) total cross sections, optical model potentials are widely used in quantum-mechanical preequilibrium and direct-reaction theory calculation. But the most important role of the optical model anaysis is to supply particle transmission coefficients for Hauser-Feshbach statistical theory anayses used in nuclear data evaluations.

In order to perform nuclear data evaluation without unphysical discontinuities, optical models should cover the whole energy range of interest continuously. Currently many optical model segments are available for the nuclear date evaluations, but most of them have been derived over very limited energy and mass regions. In the Reference Input Parameter Library (RIPL) published by IAEA [1], only Koning, Wijk and Delaroche [2] potential for neutron reactions on Zr-90 has a truly broad energy range of validity. Recently Chadwick *et al.* [3] applied Madland's global medium energy optical model [4] over wide mass and energy region. It is reported that this global potential gives a good description of measured neutron and proton cross sections for some isotopes up to 160 MeV. But it is also mentioned in the reference that the Madland's global optical potential can not reproduce in more detail the all the measured data. To supplement the Madland's global optical model, they adopted the energy dependent potential forms [5] which incorporate effects of dispersion relationship proposed by Delaroche *et al.* for some isotopes, giving better agreements with measurements. Lee *et al.* [6] also adopted the same potential form in evaluating neutron and proton cross sections of Al-27 up to 250 MeV successfully.

This work aims for a part of ground work to establish a global optical potential form having effects of dispersion relationship over wide mass range and up to 250 MeV. In this work, energy dependent optical model parameters of Delaroche type OMP were searched up to 250 MeV for some isotopes of interest: ^{12}C, ^{16}O, ^{27}Al, ^{56}Fe, ^{90}Zr and ^{208}Pb. As a byproduct, applicability of adopting an identical geometrical factor for the real volume, imaginary volume and imaginary surface potentials has been investigated as well in the process of parameter search.

2. Potential Form : Type I

The potential form factor was chosen to be of Woods-Saxon form for V_r and W_v, derivative Woods-Saxon for W_d and Thomas-Fermi form for spin-orbit parts as

$$U(r) \quad = \quad -V_r f_v(r) - i W_v \; f_w(r) + 4i \; a_{wd} \; W_d \; \frac{df_{wd}(r)}{dr}$$

$$-\frac{1}{r}\left(\frac{\hbar}{m_\pi c}\right)^2\left(V_{so}\frac{d}{dr}f_{vso}(r)+iW_{so}\frac{d}{dr}f_{wso}(r)\right)\,\boldsymbol{l}\cdot\boldsymbol{s}\,+V_{Coul}. \tag{1}$$

Figure 1 presents general shapes of potential depths of real volume(V_r), volume absorptive(W_v) and surface absorptive (W_d) adopted in this work to incorporate effects of the dispersion relationship.

$V_r(E)$ decreases exponentially down to few MeV for incident nucleon energies around 250 MeV. On the other hand. $W_d(E)$ increases to reach a plateau at around 10 MeV and then decreases smoothly with energy. W_v(E) is negligible for incident energies below 10 MeV, then increases to reach plateau at around 70 MeV.

These shapes have following functional forms:

$$
\begin{aligned}
V_r(E) &= V_0 e^{-\lambda_{vr}(E-E_f)}+V_1+V_2 E\\
W_v(E) &= W_{v0}\frac{(E-E_f)^4}{(E-E_f)^4+W_{v1}^4}\\
W_d(E) &= W_{d0}e^{-\lambda_{wd}(E-E_f)}\frac{(E-E_f)^4}{(E-E_f)^4+W_{d1}^4},\\
r_i(E) &= r_{i0}+r_{i1}E\\
a_i(E) &= a_{i0}+a_{i1}E
\end{aligned}
\tag{2}
$$

where the Fermi energy E_f for neutron and proton is given by

$$
\begin{aligned}
\text{neutron}\quad & E_f(Z,A)=-\frac{1}{2}[S_n(Z,A)+S_n(Z,A+1)]\\
\text{proton}\quad & E_f(Z,A)=-\frac{1}{2}[S_p(Z,A)+S_p(Z+1,A+1)]
\end{aligned}
\tag{3}
$$

The geometry factor of W_v is assumed to be the same as that of V_r as

$$
\begin{aligned}
r_v(E) &= r_{wv}(E)\neq r_{wd}(E)\\
a_v(E) &= a_{wv}(E)\neq a_{wd}(E)
\end{aligned}
\tag{4}
$$

Above leaves 17 adjustable parameters for the enrgy range 0 - 250 MeV of incident neutron and proton.

3. Potential Form : Type II

One thing which make this work different from all other OMP analyses is adopting the same geometry factor for all three potentials as

$$
\begin{aligned}
r_v(E) &= r_{wv}(E)= r_{wd}(E)\\
a_v(E) &= a_{wv}(E)= a_{wd}(E)
\end{aligned}
\tag{5}
$$

This reduces the number of adjusterble parameters to 13.

4. Parameter Search

The best sets of Type-I and Type-II OMP were determined by adjusting the 17 and the 13 adjustable coefficients defined in eq. (2), (4) and (5) with the use of ECISPLOT [7], an interactive optical parameter searcher with the simulated annealing algorithm, developed by the author. It is an X-Window based software system incorporated into the nuclear reaction code ECIS-96 [8]. In ECISPLOT, the potential parameters are adjusted interactively based on eye-guide, then the final parameter set is searched automatically by the simulated annealing algorithm to have minimum χ^2. During the ECISPLOT operation, smooth-varying potential depths and form factors could be collected with respect to the incident energies. With these points, rough fittings and interactive tuning were applied to get initial 17 (for Type-I) or 13 (for Type-II) coefficients. Finally, simulated annealing algorithm were applied to get the best optimum coefficient set within the ranges for each coefficient.
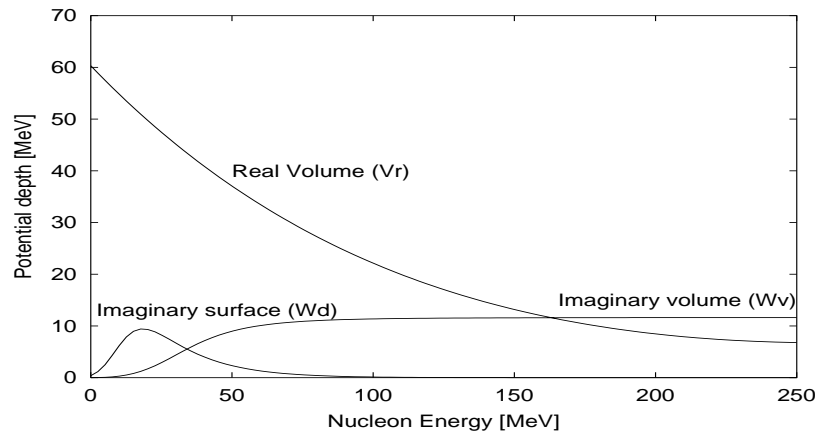
Figure 1: Depths of the real volume, imaginary volume and surface potentials as a function of incident nucleon energy

5. Results and Future Work

The total (for neutron), reaction (for proton) cross sections and elastic angular distributions resulted from Type-I OMP and Type-II OMP set are shown in Figs. 2 -7 with various measurements and LANL evaluations. Our optical model parameters give excellent agreements with most of experimental data over entire energy range for both incident neutron and proton.

Based on the results of present work, appropriate systematics will be tried to establish a global optical potential form form having effects of dispersion relationship, covering wide mass and energy range.

References

[1] Young, P. G.: *Ch4: Optical model parameters*. Tech. Rep. IAEA TECDOC-1034, International Atomic Energy Agency, Vienna, Austria (1998).

[2] Koning, A. J., *et al.*: *Neutron and proton data files up to 150 mev for 54fe, 56fe, 58ni and 60ni*. Tech. Rep. ECN-RX-97-047, Netherlands Energy Research Foundation ECN, Petten, The Netherlands (1997).

[3] Chadwick, M., *et al.*: *Nucl. Sci. Eng.*, **131**, 293 (1999).

[4] Madland, D. G.: In B. Strohmaier, ed., *Proc. of a Specialists Meeting on Preequilibrium Reactions*, no. NEANDC-245, 103–116, Paris, France (1988). Semmering, Austria, 1988, Organization for Economic Cooperation and Development (OECD) Nuclear Energy Agency.

[5] Delaroche, J., *et al.*: *Phys. Rev. C*, **39**, 391 (1989).

[6] Lee, Y., *et al.*: In *Proc. of the 1998 Symposium on Nuclear Data, Nov. 19-20, 1998, JAERI, Tokai, Japan*, no. JAERI-Conf 99-002, 246 (1999).

[7] Lee, Y.: *ECISPLOT: An interactive optical model parameter searcher with simulated annealing algorithm*. Tech. Rep. NDL-9/99, KAERI (1999).

[8] Raynal, J.: *Notes on ECIS94*. Tech. Rep. CEA-N-2772, pp. 1–145, Commisariat á l'Energie Atomique (CEA), Saclay, France (1994).
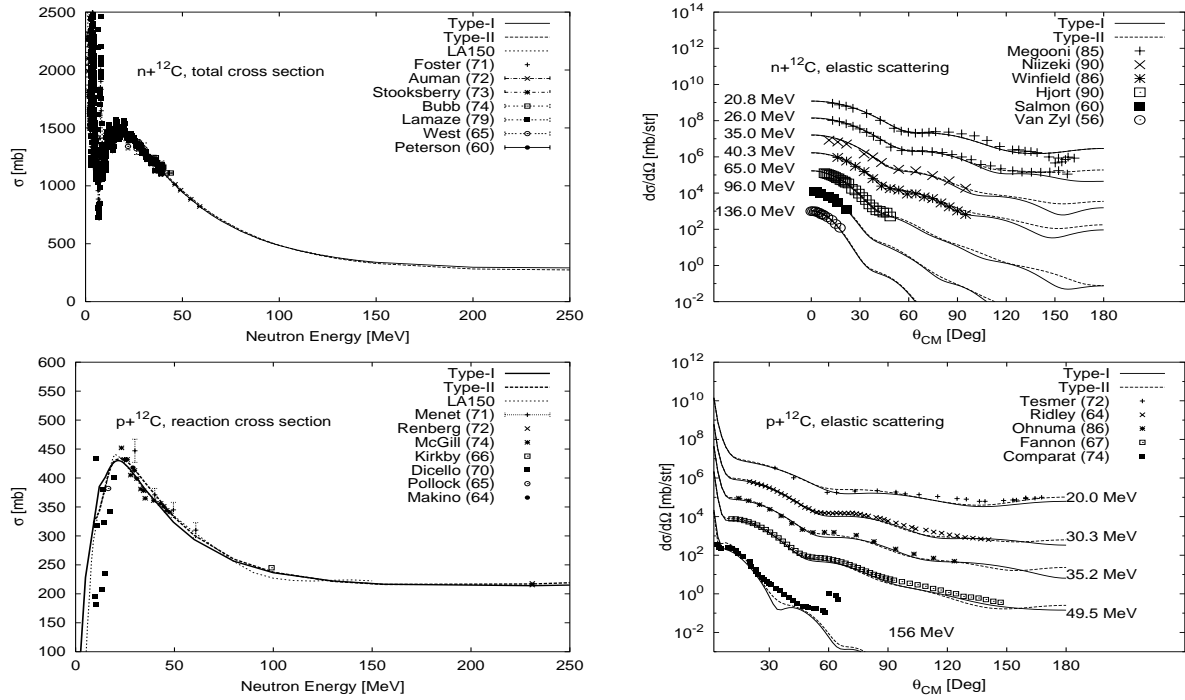
Figure 2: Total, Reaction Cross Section and Elastic Angular Distbution for n,p + ^{12}C Reactions
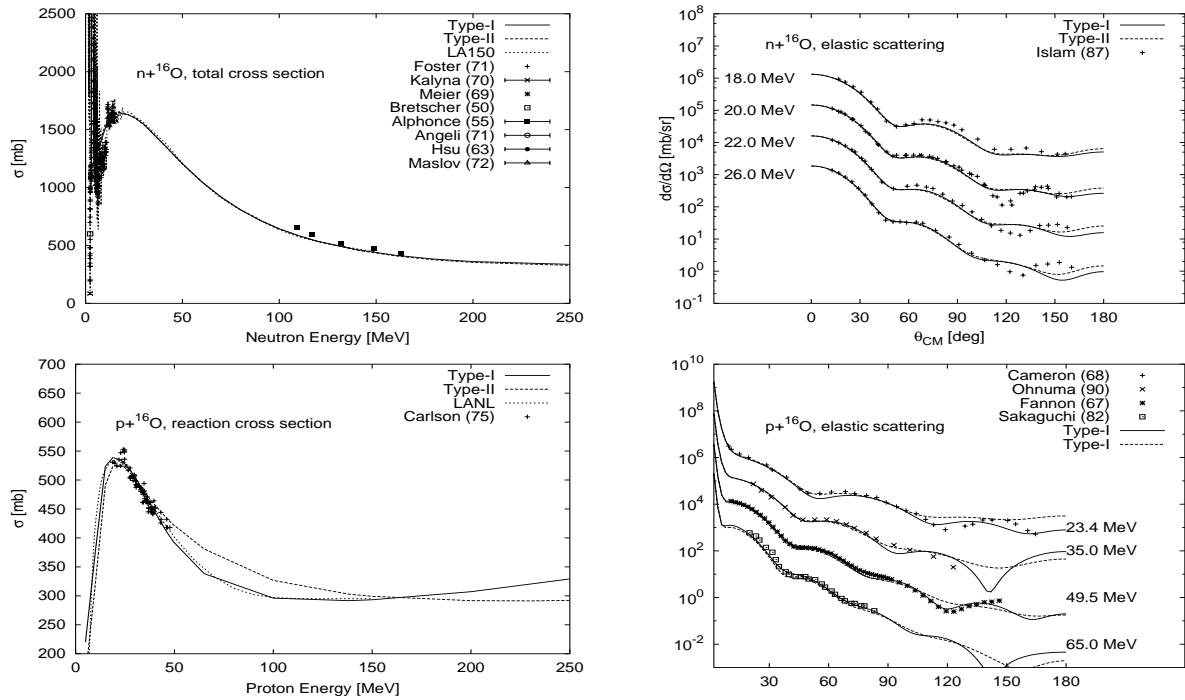
Figure 3: Total, Reaction Cross Section and Elastic Angular Distbution for n,p + ^{16}O Reactions
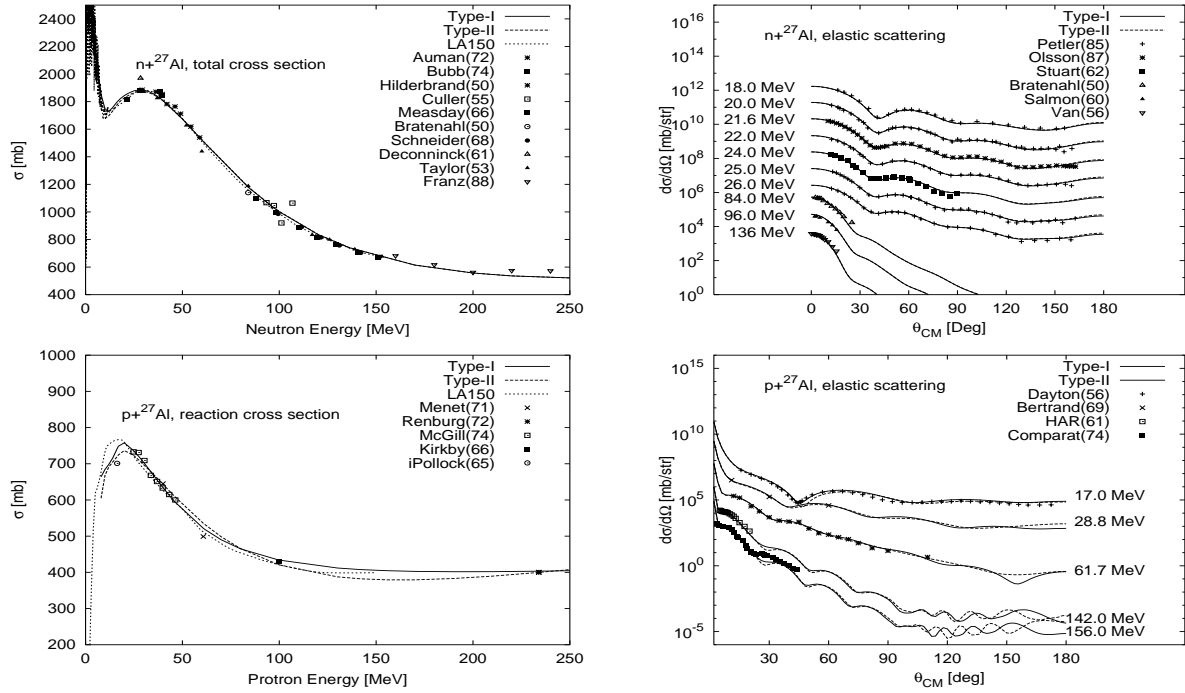
Figure 4: Total, Reaction Cross Section and Elastic Angular Distbution for n,p + ^{27}Al Reactions
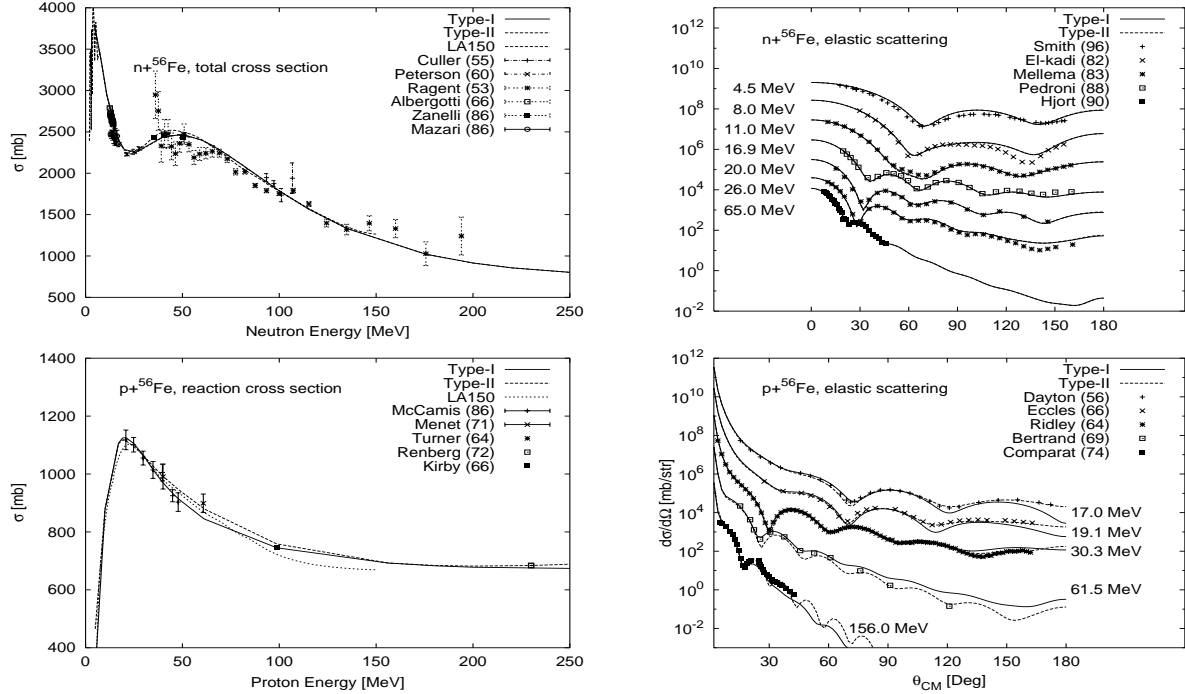
Figure 5: Total, Reaction Cross Section and Elastic Angular Distbution for n,p + ^{56}Fe Reactions
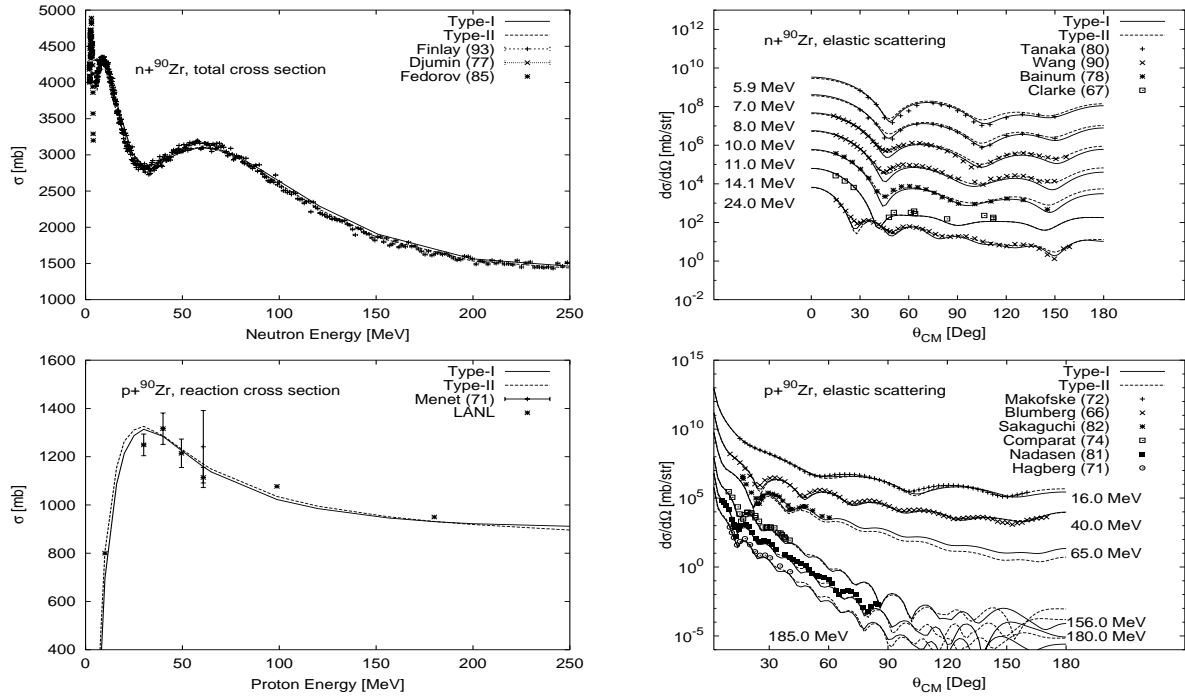
Figure 6: Total, Reaction Cross Section and Elastic Angular Distbution for n,p + ^{90}Zr Reactions
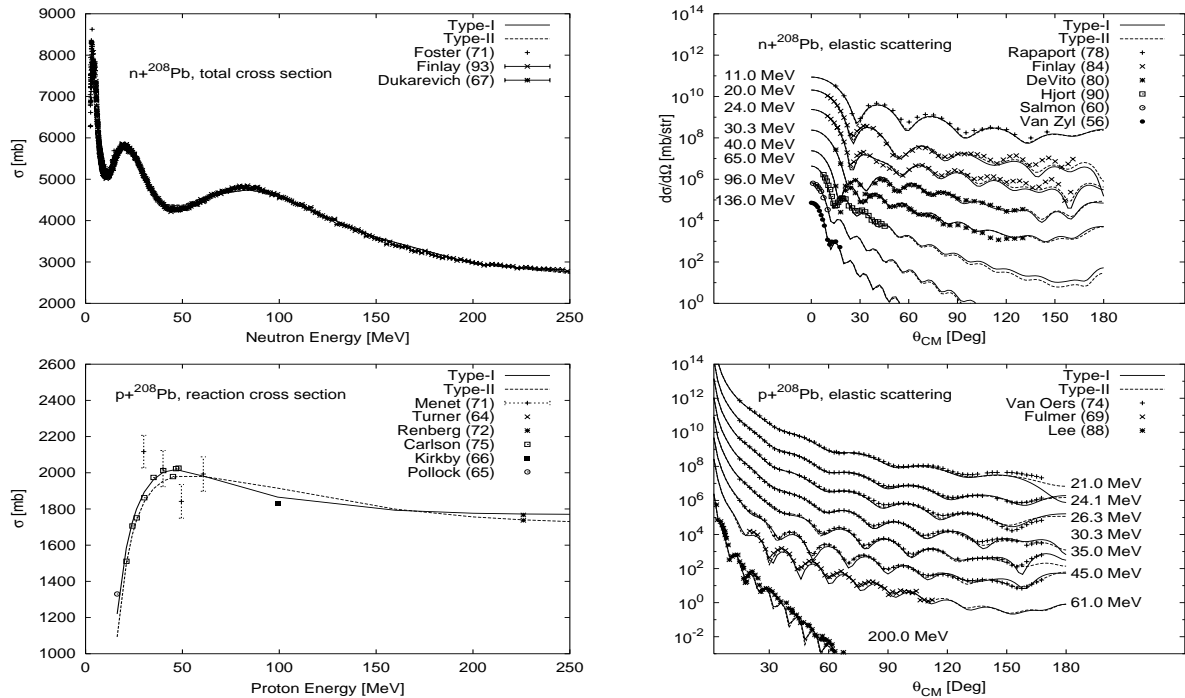
Figure 7: Total, Reaction Cross Section and Elastic Angular Distbution for n, p + ^{208}Pb Reactions